ELSEVIER

International Journal of Mass Spectrometry 198 (2000) 213–234

International Journal of Mass Spectrometry

Studies on alkali and alkaline earth chromate by time-of-flight laser microprobe mass spectrometry and Fourier transform ion cyclotron resonance mass spectrometry Part II: understanding cluster ion formation

Frédéric Aubriet, Benoît Maunit, Jean-François Muller*

Laboratoire de Spectrométrie de Masse et de Chimie Laser, IPEM, Université de Metz, 1 Boulevard Arago, 57078 Metz, Cedex 03, France

Received 17 August 1999; accepted 9 February 2000

Abstract

The formation of positively charged mixed metal oxide ions produced by alkali and alkaline earth chromate laser ablation has been investigated by Fourier transform ion cyclotron resonance mass spectrometry. The development of the fingerprints of these compounds with the increase of the counter ion radius, modification of power density, wavelength, or hydration degree allow us to gain a better understanding of the processes involved in ion formation and occurring after laser irradiation. The mixed metal ions are in all probability formed by ion/molecule reactions corresponding to sequential addition of neutral molecules on precursor ions. The ternary system of chromate compounds (chromium–oxygen–chromate counter ion) induced the presence of various neutral species in the gaseous cloud above the analyte surface; these species are responsible for the occurrence of competitive aggregation reactions. In this case, the formation of a given ion is governed by the relative affinity of its precursor ion with either neutral species. Moreover, the evolution of the alkali chromate fingerprint with the power density pushes us into considering the aggregation processes as equilibrium, the reverse way depending on the accumulated internal ion energy. By considering a simple model based on the minimization of unpaired electrons in favor of a greater stability, we additionally put forward two ionic structures for the most intense cluster ion $M_3CrO_4^+$ observed on the fingerprint of alkali chromate. (Int J Mass Spectrom 198 (2000) 213–234) © 2000 Elsevier Science B.V.

Keywords: Ion formation processes; Laser ablation/ionization; Competitive ion/molecule reactions; Cluster ions stability

1. Introduction

In the first part of this work [1] we presented the characteristic fingerprint of alkali and alkaline earth chromate, as obtained after laser ablation/ionization by time-of-flight mass spectrometry (TOF-LMMS) and Fourier transform ion cyclotron resonance mass spectrometry (LA-FTICRMS). These preliminary results allowed us to elaborate on the specific behavior of (1) alkali chromate and (2) alkaline earth chromate. An increase of the radius of the counter ion of chromate exacerbates the behavior of the two compounds. The comparison of TOF-LMMS and LA-FTICRMS fingerprints, focusing on the modification of the latter in relation with the increase of the radius

* Corresponding author.

PII S1387-3806(00)00202-5

of the chromate counter ion provided preliminary information for a better understanding of the processes involved in ion formation.

The comprehension of the mechanisms of ion formation is of prime importance from the point of view of speciation. As a matter of fact, an accurate interpretation of the results obtained by mass spectrometry will depend on notions that ought to be as accurate as possible about the processes prevailing during the formation of the cluster ions observed, so as to preclude from interpretation errors.

The study of ion formation processes after inorganic compounds laser irradiation is very critical; as a consequence, no general model—as far as we know—has been postulated up to now. However, several papers dealing with this fundamental aspect of laser-matter interaction have been published.

Hercules and co-workers [2] considered that several processes occur in several well-defined and well-separated regions at and near the laser impact. The first one is the area of direct interaction between the laser and the sample. Ionization undoubtedly occurs in this region. The high temperature reached induced an important fragmentation. This is the reason why only atomic or very little molecular species are produced in this first area. There is a second region, adjacent to the former one; it can be described as between the solid and gaseous phases. This region has a high thermal gradient, and a majority of molecularly significant ions are presumably formed there. This area is often referred as selvedge. The last region, just above the surface of the analyte, is a gaseous cloud formed by the emission of particles into vacuum by the laser impact, where ion/molecule reactions could occur. In general terms, the ions observed on the mass spectra may be, according to the model of Hercules and co-workers, simultaneously the result of laser interaction with the solid (principally atomic ions) or the product of ion/molecule reactions in the selvedge (cluster ions).

Schueler et al. [3] considered that the fast ion formation process induced by pulsed laser irradiation could not be related simply to a heating process [4]; indeed, excitation and desorption can be processes faster than thermal equilibration on the uppermost surface [3]. They concluded [5] that the cluster ion is most probably generated directly from the solid phase by disruption of the crystalline lattice. This process may be broken down into four steps: (1) irradiation of the crystal; (2) population of the conduction band (CB) by multiphoton processes in the case of alkali halides; (3) excitation of the CB electron, and (4) energy transfer to the lattice which induced the ablation process.

Dennemont et al. [6], Lafargue et al. [7], Gibson [8], Hachimi et al. [9,10], and Liu et al. [11] are amongst authors who suggested that the ion formation occurs through ion/molecule reactions in the selvedge or in the gas phase. The cluster ions may be formed by growth from smaller entities and sequential neutral molecule addition occurring on precursor ions. Some other studies seem to confirm this fact: Chaoui et al. [12] obtained similar TOF-LMMS fingerprints when $PbTiO_3$ and a PbO/TiO_2 equimolar mixture are studied successively. In the same way, Mele et al. [13] detected mixed species consistent with the empiric formula $[Cu(SrO)_n]^+$ after laser irradiation of a $CuO/SrCO_3$ mixture. Moreover, Musselman et al. [14] after analyzing natural NiS particles mounted on an isotopically enriched ^{34}S film, established the existence of ion/molecule recombination reactions in the laser-induced plasma. ^{34}S enriched cluster ions (NiS^+, NiS_2^+, and Ni_2S^+) were indeed detected. The last three cited works clearly indicate that the cluster ions observed on the mass spectra obtained do not provide information about the nature of the compound analyzed, but rather about the ion molecule reactions occurring in the laser plume after irradiation.

Recently, Liu et al. [15] published an interesting study of $Co(NO_3)_2\ 6H_2O$. Their original instrumental setup [16] allowed them to extract a selected part of the plume ions. The delay between the laser pulse and the application of the acceleration high voltage enabled them to detect the ions according to their initial transverse velocity. When the interval was very small, the cluster ions detected were only $Co_nO_m^+$. However, when the authors increased this interval, $\{Co[Co(NO_3)_2]_x\ (H_2O)_y\}^+$ cluster ions were detected. This difference is justified by differences in

initial velocity. The $\{Co[Co(NO_3)_2]_x\ (H_2O)_y\}^+$ ions are directly ejected from the sample surface, whereas the $Co_nO_m^+$ clusters ions are formed later on the free expansion by a recombination of smaller species which, due to their lower initial mass, display a higher directional velocity. Thus, Liu et al. showed that the mechanisms of cluster formation are twofold: direct ejection and ion/molecule reactions.

In the context of alkali and alkaline earth chromate, we tried to understand how major positive cluster ions are formed by laser irradiation and how the above described concepts account for the various processes taking place in the laser plume after laser ablation.

This is why we studied the fingerprint variations induced by a modification of instrumental parameters (power density and wavelength) or chemical compounds (i.e. alteration of hydration degree) before suggesting mechanisms for the formation of mixed metal oxygenated cations.

Furthermore, the study of a technical grade magnesium chromate compound containing in particular sodium impurities supplies information on the stability of the specific $M_3CrO_4^+$ cluster ions, with M being an alkaline atom. A simple model based on the minimization of unpaired electrons will allow us to confirm this fact.

The comparison of hydrated and anhydride magnesium chromate fingerprints suggested that the aggregation processes can be interpreted as competitive reactions involving the affinity of the precursor ion with each of the neutral species present in the plume after the laser irradiation.

2. Experimental

2.1. Chemicals

All chromate compounds—except for commercial technical-grade magnesium chromate (from Aldrich, Milwaukee, WI, USA)—were of analytical reagent grade and have been described in detail elsewhere [1]. Sodium nitrate (99%), potassium nitrate (99%), and rubidium nitrate (99%) were obtained from Prolabo (Paris, France).

2.2. Laser microprobe Fourier transform ion cyclotron resonance mass spectrometer

These analyses were performed using a laser microprobe FTICR mass spectrometer described in detail elsewhere [17,18]. This instrument is a modified, differentially pumped, dual-cell Nicolet Instrument FTMS 2000 (Finnigan FT/MS, now named ThermoQuest, Madison, WI, USA) operated with a 3.04 tesla magnetic field and coupled to a reflection laser interface.

The viewing system, using an inverted Cassegrain optics design, allows one to visualize the sample with 300-fold magnification. A new sample probe fitted with motorized three-dimensional (3-D) micromanipulators allows spatial accuracy values of less than 10 μm.

The ionization step was performed using the third harmonic of a Nd-YAG laser (λ = 355 nm, pulse duration 4.3 ns, output energy used 0.8 mJ). Alternatively, an excimer laser charged with an ArF mixture (λ = 193 nm, pulse duration 23 ns, output energy used 1.6 mJ) was used. The diameter of the laser beam on the sample (placed inside the source cell) can be adjusted by means of the internal lenses and an external adjustable telescope from 5 μm to several hundred μm, which corresponds to a power density ranging from 10^{10} to 10^6 W/cm^2.

The experiment sequence used for these analyses has been described in the first part of this study [1]. It should be noted that all experiments were performed with Cr^+ and M^+ ejection [19] (where M is the counter ion of the chromate compounds) in order to enhance the detection of the signal supplied by mixed oxygenated cluster ions. In fact, the majority of atomic ions induces a dissociation of cluster ions by collision and disturbs the detection process. Each FTICR mass spectrum resulted from an average of one hundred laser shots fired on consecutive spots.

3. Results and discussion

In the second part of this study we examine the influence of instrumental parameters on the mass spectra obtained.

Two specific laser parameters induce fingerprint modifications. The power density dependence prevails over the mass spectra obtained in positive and negative detection modes from 10^7 to 10^{10} W/cm^2. Similarly, laser wavelength variation induces changes in the fingerprints.

Only the study of the mixed metal ions observed in positive detection mode will be presented. Indeed, this kind of ions are in small numbers in the negative detection mode, the major part of the negative mass spectra is composed of pure oxygen–chromium ions [1]. Moreover, the results refer to the influence of the hydration degree on the fingerprint of magnesium chromate compounds will equally be presented.

3.1. Influence of experimental parameters

3.1.1. Influence of power density on the fingerprint of alkali chromate at wavelength 355 nm

The development of the fingerprints displayed by the five alkali chromate compounds in relation to power density is, all in all, similar. Only minor differences appeared when we compared the relative ion distribution of these five compounds. As already shown [1], the stability of the ion is reinforced as the radius of the alkali increases. Consequently, the ratio between the intensity of other $M_nCr_xO_y^+$ to $M_3CrO_4^+$ ions significantly decreases when lithium, sodium, potassium, rubidium, and cesium are successively studied by mass spectrometry. As a consequence, in this part of the study, we provide only the results obtained with sodium chromate, considering that those supplied by the other alkali chromate compounds—except for lithium chromate—are similar.

Qualitatively, for all power densities, the same cluster ions are produced after laser irradiation of sodium chromate. Nevertheless, major changes in relative intensity occur [Figs. 1(a) and 1(b)]. At high power density, between 5×10^8 and 4×10^{10} W/cm^2, the largest part of the ions produced display roughly the same relative intensity, whereas, at lower power density in the 5×10^7–5×10^8 W/cm^2 range, we observed an significant decrease of all relative intensities except for $M_3CrO_4^+$. Moreover, the absolute $M_3CrO_4^+$ intensity, in this same power density range, increases strongly to approximately 20 times the value observed at high power density [Fig. 2(a)].

Globally, the significant decrease in relative intensity observed with the majority of the cluster ions results from a greater production of $M_3CrO_4^+$ ions. This may be related to the particularly great stability of this ionic structure [1].

When the power density is further reduced to reach the ablation threshold at approximately 10^7 W/cm^2, we simultaneously observed that, even if this ion remained the main ion on the mass spectra, the absolute intensity [Fig. 2(a)] of $M_3CrO_4^+$ ions decreased whereas that of the other ions increased [Figs. 1(a) and 1(b)]. This development—running parallel to the other one—is to be assigned to the same effect: a lower yield of $M_3CrO_4^+$ ions. A decrease in power density induces indeed a reduction of the neutrals and ionic species produced by chromate compounds laser irradiation. The very poor abundance cluster ions are relatively little affected by this fact whereas the major $M_3CrO_4^+$ cluster ions are strongly influenced by a small quantity of neutrals and ionic production.

Furthermore, the general evolution of ion relative intensity showed that there was higher mixed metal production at low power density. The number of ions with more than one chromium atom in their structure increases when the power density is in the 10^7–5×10^8 W/cm^2 range [Fig. 1(b)]. That may be assigned, first to a greater production of oxygenated neutrals and ionic species formed by ion/molecule reactions involving cluster metal ions, and second to a lower photon density in the gaseous plume. The cluster ions formed consequently store less internal energy and then undergo less dissociative processes. In other words, in an optimal power density range, the photon density is adequate to induce enough neutral and ionic species and to limit dissociation processes by energetic excess.

As noted above, the behavior of potassium, rubidium, and cesium chromate with respect to power

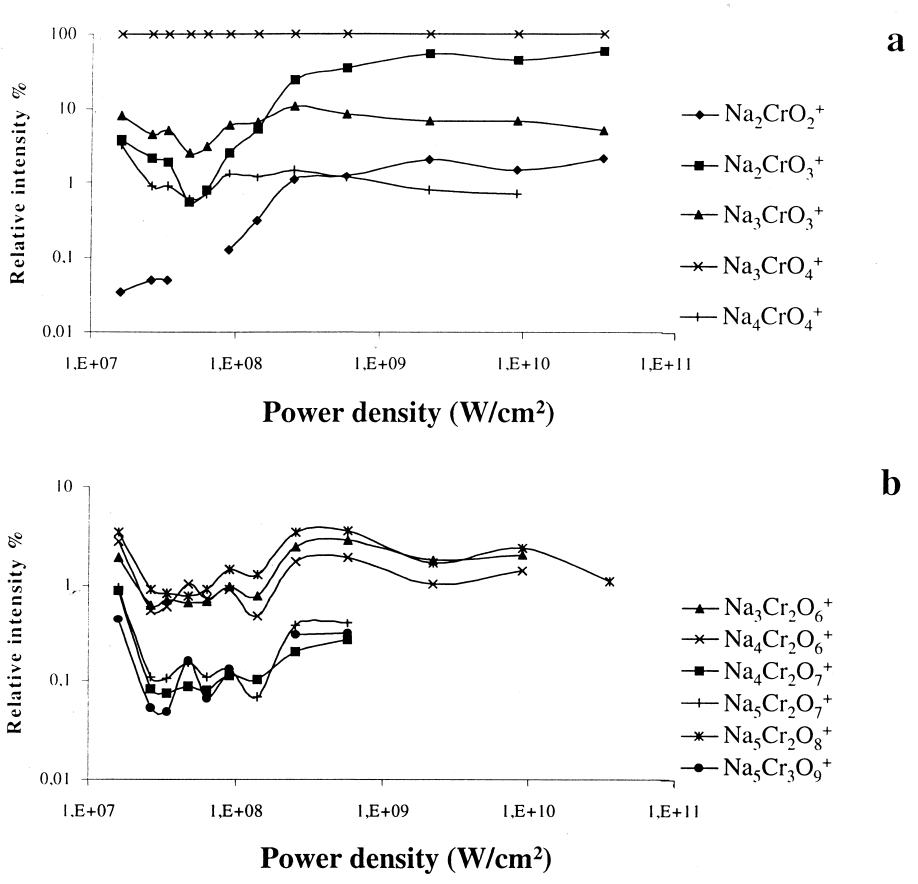

Fig. 1. Development of the FTICRMS fingerprint of sodium chromate in the 10^7–4×10^{10} W/cm^2 power density range, at wavelength 355 nm. Distribution of mixed metal oxygenated ions (a) with only one chromium atom and (b) with at least two chromium atoms.

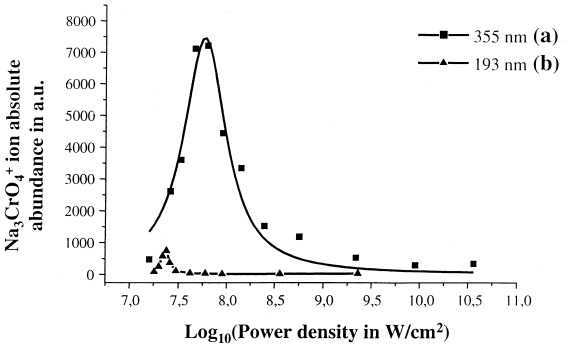

Fig. 2. Evolution of $Na_3CrO_4^+$ absolute intensity in the 10^7–4×10^{10} W/cm^2 power density range, at (a) 355 or (b) 193 nm.

density is identical to that of sodium chromate, whereas that of the lithium compound is slightly different.

A systematic study of alkali chromate compounds allows one to establish that the differences in stability between the various mixed metal cluster ions are less important with the lithium–chromium–oxygen species than the other alkali ones. The evolution of the fingerprint of lithium chromate with power density is original [Fig. 3(a) and 3(b)]. According to the power density used, the major ion is the $Li_3CrO_4^+$ cation at high ($>10^9$ W/cm^2) or low ($<2 \times 10^7$ W/cm^2) power density, whereas it is the $Li_3CrO_3^+$ cation in the intermediate power density range. Moreover, the difference in relative ion intensity between the various

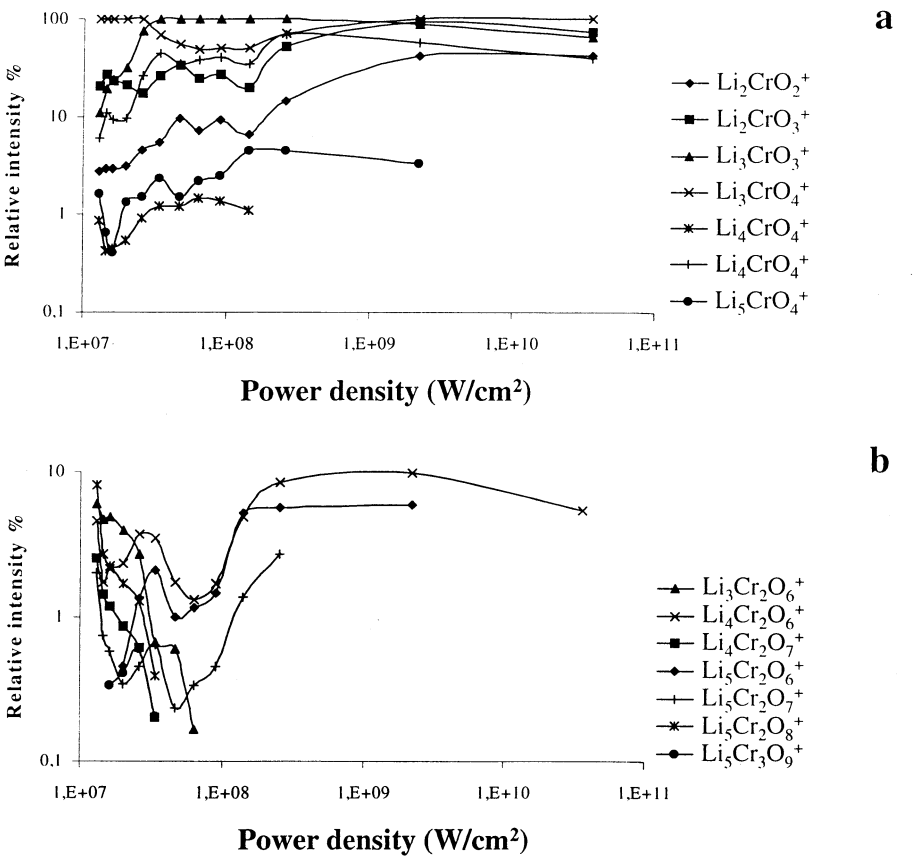

Fig. 3. Evolution of the FTICRMS fingerprint of lithium chromate in the 10^7–4×10^{10} W/cm^2 power density range, at wavelength of 355 nm. Distribution of mixed metal oxygenated ion (a) with only one chromium atom and (b) with at least two chromium atoms.

ions is less significant in the case of lithium chromate fingerprints. All these facts testify to a lesser difference in stability between all the cluster ions produced by laser irradiation of the lithium chromate compounds, as compared to what was observed when studying the other alkali chromate. The detection of 14 mixed metal cluster ions on the Li_2CrO_4 fingerprint, as against 6 detected with Cs_2CrO_4 seems to support this conclusion [1].

3.1.2. Influence of wavelength when varying between 355 and 193 nm

As in Sec. 3.1.1, we focused on the results obtained after laser irradiation of the sodium chromate compounds at 193 nm in the power density range of 5×10^9–10^7 W/cm^2. The evolution of the fingerprint with the power density at 193 nm is comparable to what was observed at 355 nm [Figs. 2(b) and 4].

The absolute intensity of $Na_3CrO_4^+$ is almost constant over the whole power density range, except between 2×10^7 and 3×10^7 W/cm^2; in this specific case, the absolute $Na_3CrO_4^+$ intensity increases by a factor of 7 [Fig. 2(b)], whereas, at the same time, the relative intensity of the other ions decreases significantly [Figs. 4(a) and 4(b)]. In the latter case, as at a wavelength of 355 nm, the optimum power density value has to be reached to yield the $Na_3CrO_4^+$ ion.

However, some differences appear when examining the detail of the results obtained. Indeed, we noticed first that there was a shift of the optimum formation power density for $Na_3CrO_4^+$ and second a significant decrease of its absolute intensity when

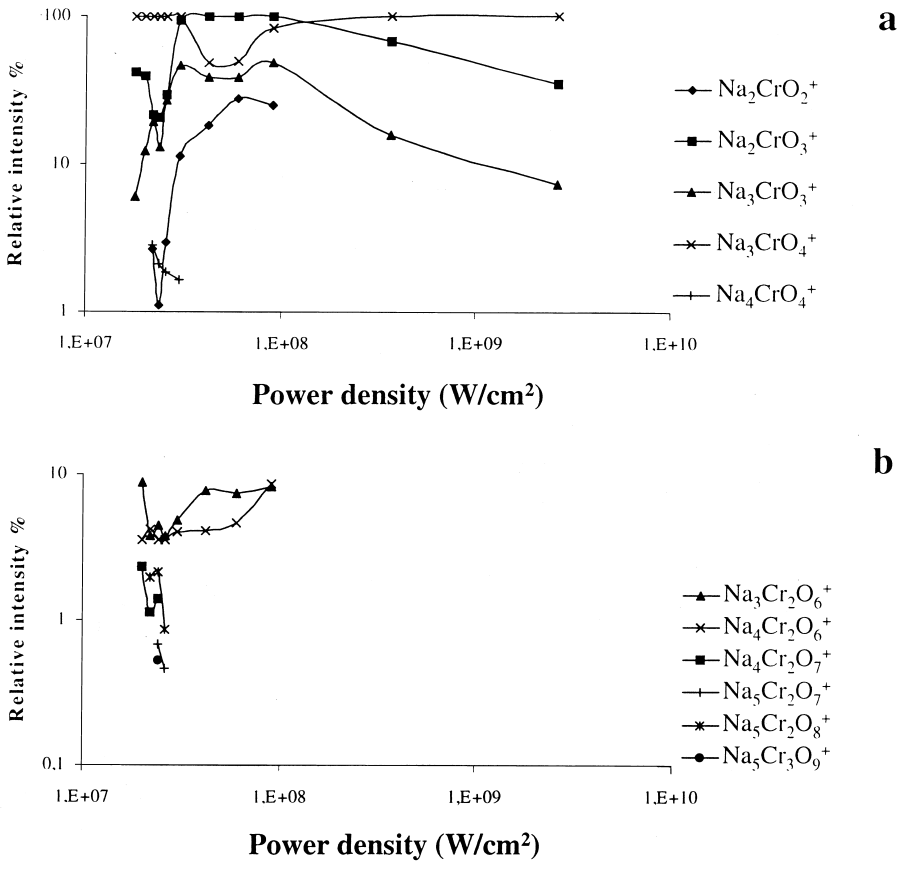

Fig. 4. Evolution of the FTICRMS fingerprint of sodium chromate in the 10^7–5×10^9 W/cm^2 power density range, at wavelength of 193 nm. Distribution of mixed metal oxygenated ion (a) with only one chromium atom and (b) with at least two chromium atoms.

sodium chromate was studied at wavelengths of 355 and 193 nm.

To understand these behaviors, we can make various suggestions. First, the absorbance of sodium chromate at 193 and 355 nm: it appears clearly in Fig. 5 that the absorbance is three times weaker at 193 nm than at 355 nm. Consequently, we may reasonably consider that the ablation process is more effective at the latter wavelength and more neutrals and ionic species are ejected from the sodium chromate after laser irradiation. The higher absolute intensity of the $Na_3CrO_4^+$ ion at 355 nm may also be assigned to two laser parameters: the pulse duration and the photon energy (Table 1). At 193 nm, a greater value of energy per photon and a longer pulse duration are more

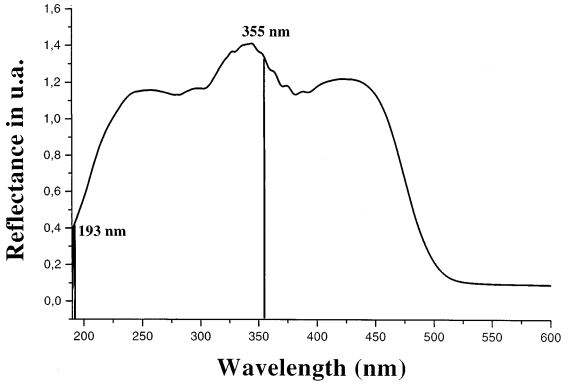

Fig. 5. Solid phase absorbance spectra obtained for sodium chromate UV–VIS; barium sulfate is taken as reference material.

Table 1
Parameters of laser equipment

Wavelength (nm)	193	355
Pulse duration (ns)	23	4.3
Energy per photon (eV)	6.42	3.49

favorable for the storage of ion internal energy by multiphoton processes, considering that the excess of internal energy induces cluster ion fragmentation. Finally, the same arguments may be evoked to account for a shift in the optimum formation power density of $Na_3CrO_4^+$ ions. We may consider that, at 193 nm, the energy required to induce a dissociation of $Na_3CrO_4^+$ ionic structure a lower photon density and, consequently, a lower power density. Furthermore, the pulse duration at 193 nm is five times longer than at 355 nm (respectively, 23 and 4.3 ns, Table 1). Thus, at comparable power density, the probability to have a multiphotonic absorption process favorable to dissociative pathway is higher at 193 nm.

Moreover, it is interesting to observe the specific behavior of $Na_2CrO_3^+$ and $Na_3CrO_4^+$ cluster ions under various power densities. At 355 nm, ion with the highest intensity was always the $Na_3CrO_4^+$ one, whereas $Na_2CrO_3^+$ becomes the most intense ion in the 3×10^7–9×10^7 power density range when the experiments are carried out at wavelength 193 nm [Fig. 4(a)].

This behavior should be accounted for to understand the pathway of $M_3CrO_4^+$ ion formation processes. This is the reason why we tried to provide a solution to the delicate issue of cluster ion formation.

3.2. Studying the formation processes of $M_3CrO_4^+$ ions

Two hypotheses should be taken in account for the formation process of $M_3CrO_4^+$ ions during the laser ablation of alkali chromate compounds.

The first one consists in M_2CrO_4 molecular desorption, followed by the cationization of this neutral structure

$$M_2CrO_4 + M^+ \rightarrow M_3CrO_4^+ \quad (1)$$

The second one corresponds to a stepwise adduction of neutrals to a precursor ion

$$CrO_4^{2-} \xrightarrow{M^+} MCrO_4^- \xrightarrow{M^+} M_2CrO_4 \xrightarrow{M^+} M_3CrO_4^+ \quad (2)$$

and

$$CrO^+ \xrightarrow{MO} MCrO_2^+ \xrightarrow{MO} M_2CrO_3^+ \xrightarrow{MO} M_3CrO_4^+ \quad (3)$$

In this case, we can consider two different processes: (1) a stepwise adduction of three alkali M^+ ions on the discharged CrO_4^{2-} anion equation (2), or (2) a sequential MO neutral adduction to the CrO^+ precursor ion equation (3).

3.2.1. First hypothesis: neutral molecular desorption, followed by alkali cationization

It can be assumed that there is first laser interaction with the analyte leading to a desorption of intact analyte molecules, and second alkali cationization of these molecular neutrals by a positive alkali ion formed by the laser ablation of the compound analyzed.

This first formation pathway is comparable to the matrix-assisted laser desorption ionization ion formation processes. Some experimental results seem to confirm this assumption: first, the fact that highest production of $M_3CrO_4^+$ ions occurs when power density values range between 10^7 and 10^8 W/cm^2, depending on the alkali chromate compound studied. This power density range corresponds approximately to the best conditions in organic laser ablation/ionization mass spectrometry to obtain the desorption of molecular structures. Second, the alkali M^+ ions produced, at whatever power density, make up an important stock of cationizing ions. Finally, Rudny et al. [20] showed with a Knudsen effusion cell coupled to mass spectrometry that gaseous molecules of potassium chromate are present above the surface of K_2CrO_4 heated up at 1215 K. In the 10^7–10^8 W/cm^2 power density range, the temperature at the surface of

the analyte exceeds this value and we may reasonably think that $K_2CrO_4(g)$ is produced during the laser ablation of this compound by thermal exchange processes.

However, several considerations tend to discard this assumption on the process of ion formation: first, the intensity of $M_3CrO_4^+$ cluster ions is very weak at high power density values though the experimental conditions are in favor of an important production of M_2CrO_4 molecules by sublimation, as the surface of the analyte compound pellet undergoes a high overheating at laser impact. Furthermore, the ratio of ionic to neutral species is higher at high power density; the production of M^+ ions is therefore more important. In general terms, the production of $M_3CrO_4^+$ ions by the ion/molecule reaction between sublimated M_2CrO_4 and M^+ ions is theoretically favored at high power density. Experimentally, the greatest production of $M_3CrO_4^+$ ions is obtained in a lower range of power densities (Fig. 2).

Finally, the results obtained by mass spectrometry on alkali nitrate—alkali chromate compound mixtures shown in Fig. 6 provide additional evidence against this assumption.

Thus, this hypothesis is not appropriate to account for all experimental results. To bring this part of the study to a successful conclusion, we considered six alkali chromate M_2CrO_4—alkali nitrate $M'NO_3$ mixtures, where M and M′ are sodium, potassium, or rubidium, but M and M′ are different for a given mixture.

The mixed samples were prepared by grinding an equimassic mixture of nitrate and chromate compounds in an agate mortar for 15 min. To limit the number of experiments, we processed only the sodium, potassium, and rubidium compounds. We removed the lithium and the cesium ones for two reasons: first, $^6Li^+$ and $^7Li^+$ are submitted to the foldover effect [1] and induce unnecessary difficulties for interpretation and second, the introduction of cesium compounds into our instrument is a cause of long-term pollution. An intense signal at *m/z* 133 corresponding to the Cs^+ ion endures on mass spectra for a long time after studying these cesium compounds.

If hypothesis (1) were true, only two ionic structures should be formed. When mixing the chromate M_2CrO_4 and nitrate $M'NO_3$ compounds, we indeed obtain one chromate molecule source: M_2CrO_4, and two alkali ions sources: M^+ and M'^+. Consequently, according to hypothesis (1), only $M_3CrO_4^+$ and $M_2M'CrO_4^+$ ions should be produced by the following two processes

$$M_2CrO_4(subli) + M^+(g) \rightarrow M_3CrO_4^+(g) \quad (4a)$$

$$M_2CrO_4(subli) + M'^+(g) \rightarrow M_2M'CrO_4^+(g) \quad (4b)$$

Experimentally, two types of cluster ions are obtained, the first ones are $M_xM'_{3-x}CrO_4^+$ with $x = 0–3$, and the second ones are $M_xM'_{5-x}Cr_2O_8^+$ with $x = 0–5$. These two ionic structures are considered [1] as the most stable ones in the studies on pure alkali chromate. We will address only to the former one.

Contrary to expectations, the two $M_2M'CrO_4^+$ and $M'_3CrO_4^+$ ions are also detected. For example, in the mass spectrometric study of the K_2CrO_4–$RbNO_3$ and Rb_2CrO_4–KNO_3 mixtures [Figs. 6(e) and 6(f)], all $M_xM'_{3-x}CrO_4^+$ combination ions are detected: $K_3CrO_4^+$; $K_2RbCrO_4^+$; $KRb_2CrO_4^+$, and $Rb_3CrO_4^+$. These experimental results cannot be accounted for by cationization of the desorbed neutral molecule. These results suggest that the hypothesis (1) should be ruled out.

Moreover, these experiments on alkali exchange allow us to put forward various considerations. First, when doing mass spectrometric investigation on alkali chromate, the processes of ion formation are ion/molecule reactions taking place between alkali and chromium species in the laser ablation plume. Second, the stepwise blending of three alkali species from the nitrate compound allow us to establish that the formation of the $M_3CrO_4^+$ occurs via successive reactions.

Finally, these experiments confirm the conclusions obtained in the first part of this work [1] concerning the relative stability of the $M_3CrO_4^+$ ions when the five alkali chromate compounds are successively studied. In all cases, when the electronegativity of the alkali atoms in the nitrate compound is lower than that of chromate, we observe that there is an important ion

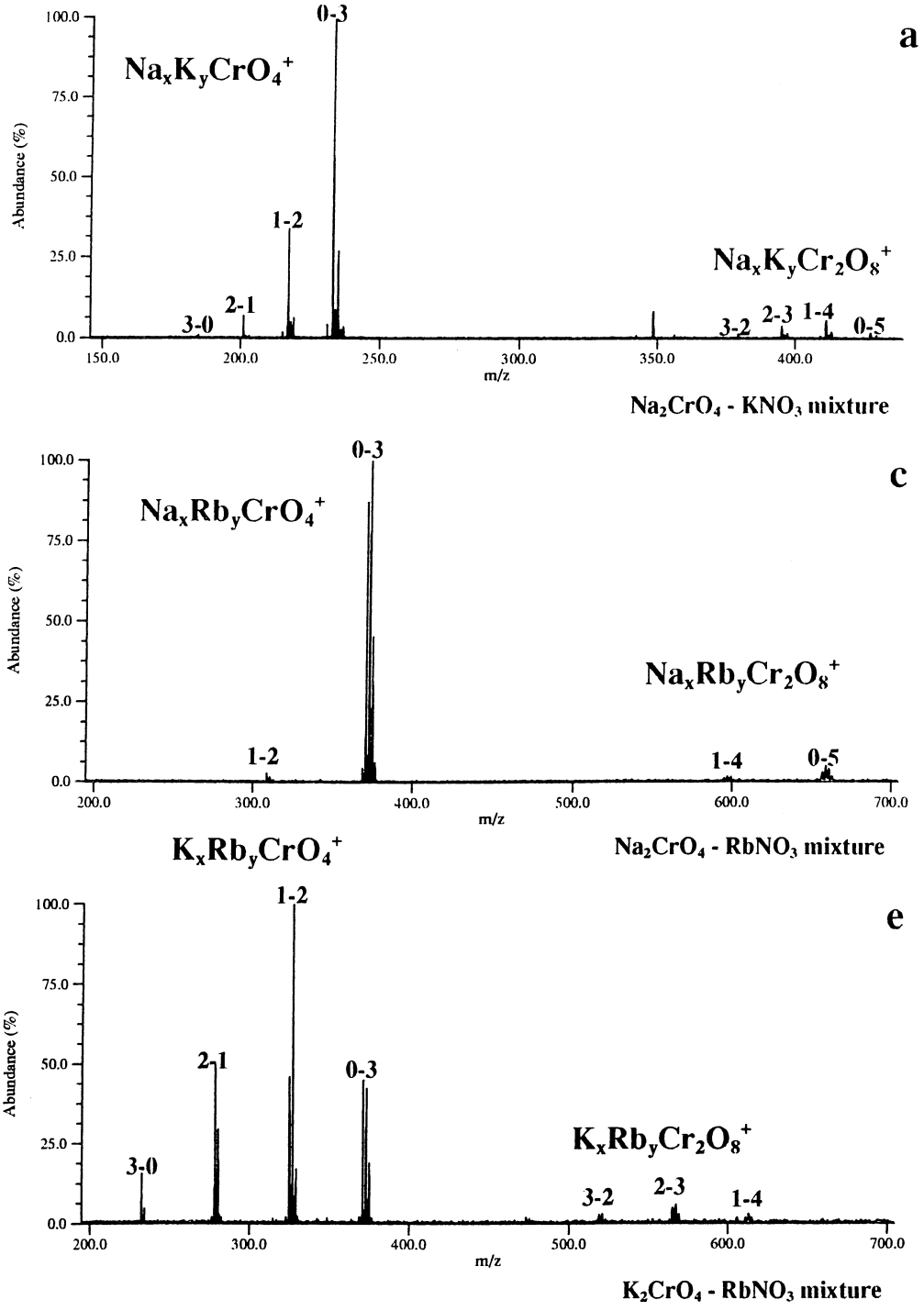

Fig. 6. FTICRMS examination of alkali chromate–alkali nitrate equimassic mixtures (a) Na_2CrO_4–KNO_3, (b) K_2CrO_4–$NaNO_3$, (c) Na_2CrO_4–$RbNO_3$, (d) Rb_2CrO_4–$NaNO_3$, (e) K_2CrO_4–$RbNO_3$, and (f) Rb_2CrO_4–KNO_3 at 355 nm with a power density of 5.4×10^7 W/cm^2.

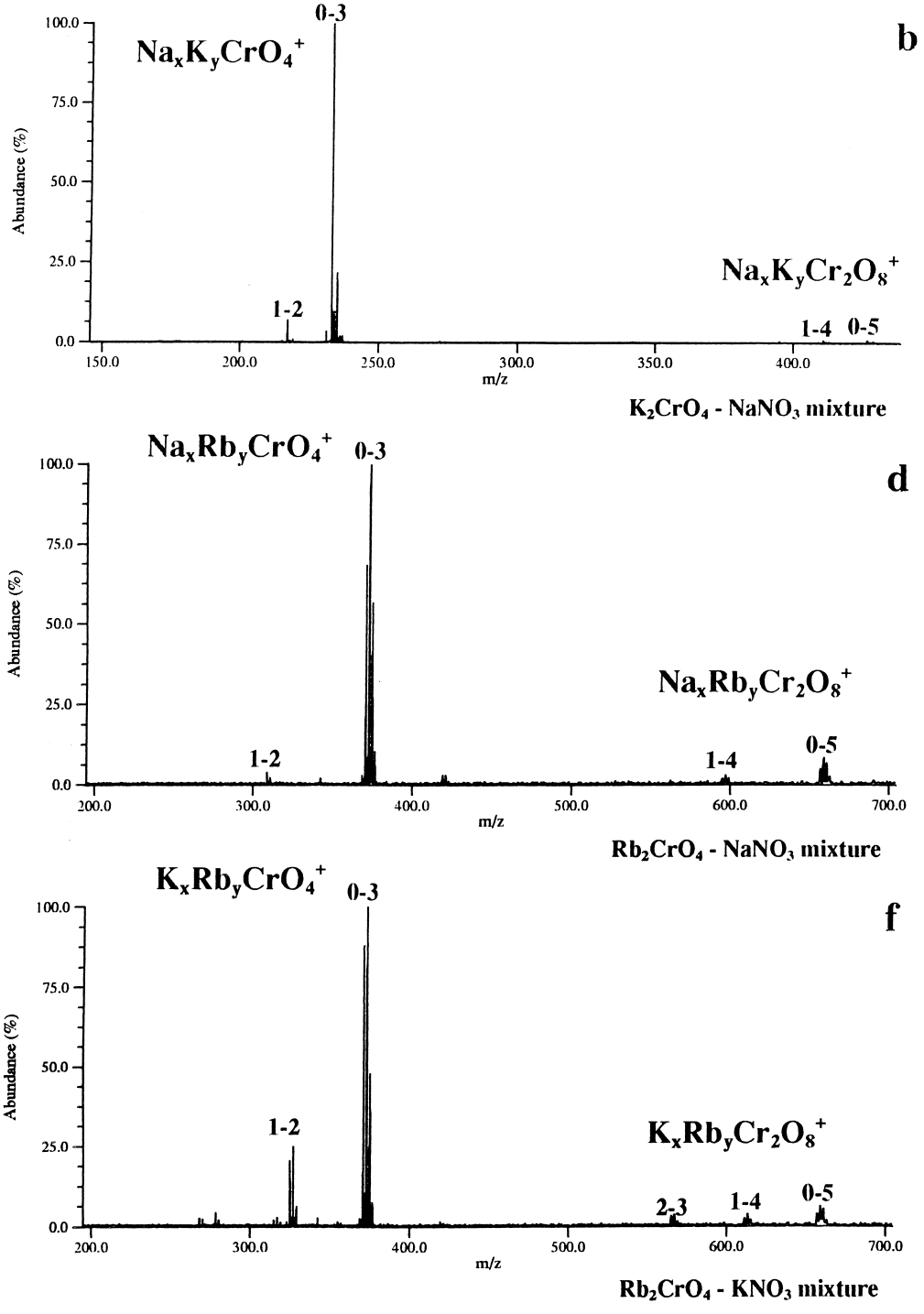

Fig. 6. Continued.

Table 2
Molecular ratio *R* of alkali from nitrate compound to alkali from chromate

	Nitrate compounds		
Chromate compounds	$NaNO_3$	KNO_3	$RbNO_3$
Na_2CrO_4	...	0.80	0.55
K_2CrO_4	1.15	...	0.60
Rb_2CrO_4	1.70	1.42	...

exchange [Figs. 6(a), 6(c), and 6(e)], and the mass spectra obtained are composed of mixed alkali cluster ions. Conversely [cf. Fig. 6(b), 6(d), and 6(f)], when the electronegativity of alkali atoms is lower in the chromate than in the nitrate compound, the mass spectra obtained are similar to those observed when studying pure alkali chromate compounds [1]; only mixed alkali cluster ions are then detected in poor abundance. Further, the greater the difference in electronegativity between the atoms of nitrate and chromate alkali is, the more visible these behaviors are. For example, when studying mixtures including sodium and rubidium compounds, the majority of ions obtained are in both cases (sodium nitrate–rubidium chromate and sodium chromate–rubidium chromate mixtures) pure rubidium/chromium oxygenated $Rb_3CrO_4^+$ and $Rb_5Cr_2O_8^+$ ions [Figs. 6(c) and 6(d)]. The ions including a sodium atom are indeed in small quantities.

These experiments prove that the electronegativity of alkali atoms and their relative affinity for oxygen are important factors for the processes of ion formation.

The difference observed between the spectra on, respectively, Figs. 6(a) and 6(b), and 6(e) and 6(f) can be accounted for by the calculation of the molecular *R* ratio

$$R = \frac{n_{M'_{nitrate}}}{n_{M_{chromate}}} \quad (5)$$

between the alkali atoms from the nitrate and chromate compounds (Table 2). In all cases, this ratio is higher when the nitrate with the largest amount of electronegative alkali is mixed with the alkali chromate having lowest electronegativity. For example, this ratio is higher twice in the case of Rb_2CrO_4–KNO_3 mixtures, as compared to that of K_2CrO_4–$RbNO_3$, this difference justifies why, in the case shown in Fig. 6(e), the $Rb_3CrO_4^+$ is not the main ion, contrary to what was obtained in the second case shown in Fig. 6(f).

Though the ratio *R* is important for the relative distribution observed on the mass spectra, it is not the only parameter to be considered that accounts for the difference observed between the spectra, respectively, shown on Figs. 6(a) and 6(b), 6(c) and 6(d), and 6(e) and 6(f). Indeed, if we compare the two spectra described on Fig. 6(c) and 6(d), we observe similar relative distribution of ions—with minor differences—whereas the ratio *R* of the mixture studied in Fig. 6(c) is three times higher than that in Fig. 6(d). In the latter case, the thermodynamic effect (difference of oxygen affinity), which is responsible for the formation of the $Rb_3CrO_4^+$ ions, is too strong to allow the observation of the less stable $Na_xRb_{3-x}O_4^+$ ionic structures (with $x \neq$ zero).

The progressive introduction of alkali atoms from the nitrate compound into the $M_3CrO_4^+$ ionic structure suggests that the formation of this cluster ion may be the result of successive adducts on a precursor specie.

Two different processes may be mentioned: the stepwise adduction of three metal ions M^+ on the CrO_4^{2-} precursor anion (2), or the successive adduction of neutral MO on the CrO^+ ion (3).

3.2.2. Second hypothesis: aggregative processes of M^+ metal ions on the CrO_4^{2-} precursor ion:

$$CrO_4^{2-} \xrightarrow{M^+} MCrO_4^- \xrightarrow{M^+} M_2CrO_4 \xrightarrow{M^+} M_3CrO_4^+$$

The detection of $MCrO_4^-$ for all alkali chromate compounds in mass spectrometry investigations in the negative detection mode tends to confirm this process [1]. Nevertheless, we never detected the CrO_4^{2-} anions, but this fact should not be taken as an refutation of the assumption. We may, indeed, consider that the first step is very fast, and the time required for $MCrO_4^-$ ion formation may be considerably lower than the time interval between the generation by laser

ablation/ionization of the ions and these ions are detected.

However, other observations suggest that this process of $M_3CrO_4^+$ ion formation is very improbable.

First, with FTICRMS equipment, the detection of positive ions is ensured by the application of positive potentials to the trapping plates to maintain them inside a potential well. The presence of negative ions between the two trapping plates is possible only during the very short time interval between their formation and the collision with either of the trapping plate. In other words, the first two steps of process (2) may kinetically occur very swiftly before the negative ions disappear. Moreover, the presence of neutral M_2CrO_4 molecules that are not trapped by the potential application on the pathway of ion formation is another limitation to this process.

The key point of process (2) is the formation of CrO_4^{2-} precursor ions. Indeed, the formation of multicharged species by laser ablation in our instrumental conditions is very unusual. With our equipment, only few experiments made possible the detection of multicharged ions. This occurred only at very high power density ($>10^{10}$ W/cm^2) and it provided only atomic species, whereas the highest yield of $M_3CrO_4^+$ ions took place at lower power density (between 10^7 and 10^8 W/cm^2). However, two CrO_4^{2-} ion formation pathways may be considered. The first one is consistent with a double electronic capture

$$CrO_4 \xrightarrow{e^-} CrO_4^- \xrightarrow{e^-} CrO_4^{2-} \quad (6)$$

and the second one consists in a photodissociation of the ionic bounds in the chromate structure under the laser beam

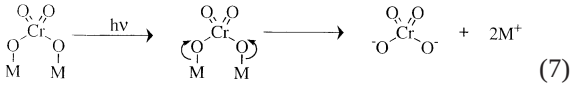

(7)

The electronic affinity of CrO_4^- is equal to −85 kJ/mol [20]; it is therefore not favorable to this process in the laser plume.

To investigate the capacity of process (7) to account for the formation of the CrO_4^{2-} anion, a comparative investigation of the potassium chromate and bichromate TOF-LMMS fingerprints was carried out (Fig. 7). Whereas CrO_4^{2-} ions were obtained by K_2CrO_4 laser ablation when applying reaction (7), the same type of process applied to the $K_2Cr_2O_7$ would reasonably produce the $Cr_2O_7^{2-}$ ion in the following process:

$$K_2Cr_2O_7 \xrightarrow{h\nu} 2K^+ + Cr_2O_7^{2-} \quad (8)$$

In this case, the precursor ion would be $Cr_2O_7^{2-}$, and, by a process similar to reaction (2), the cluster ion in a majority should be $K_3Cr_2O_7^+$.

Experimentally, when we compared the TOF-LMMS fingerprints of potassium chromate [Fig. 7(a)] and bichromate [Fig. 7(b)], no difference was observable. In both cases, the main cluster ion detected is $K_3CrO_4^+$. However, we observed a dramatic decrease of $(KO)_n\ Cr^+$ intensity ($n = 2$ or 3); this result may be considered as revealing the greater stability of $(KO)_nCrO^+$ ions, as compared to $(KO)_nCr^+$ ions, and it may be related to the disappearance of the latter species on the FTICRMS fingerprints of alkali chromate [1].

The aggregation pathway (2) may be rejected for another reason. The process of negative ion formation when studying these compounds in our experimental conditions is weakly influenced by changes in wavelength; as a matter of fact, no notable changes appeared in the fingerprints on negative mass spectra between 193 and 355 nm. Thus, the yield of CrO_4^{2-} ions should not be notoriously altered when alkali chromate compounds are successively investigated at 355 and 193 nm. Moreover, the production of atomic ions increases at the latter wavelength; it can be seen that, whereas the ionization of alkali atom—with the exception of cesium—calls for two photons at 355 nm, only one is necessary to induce photoionization at 193 nm.

In general terms and with due account for the above two points, the formation of the $M_3CrO_4^+$ ion is not likely to be greatly modified by a variation in

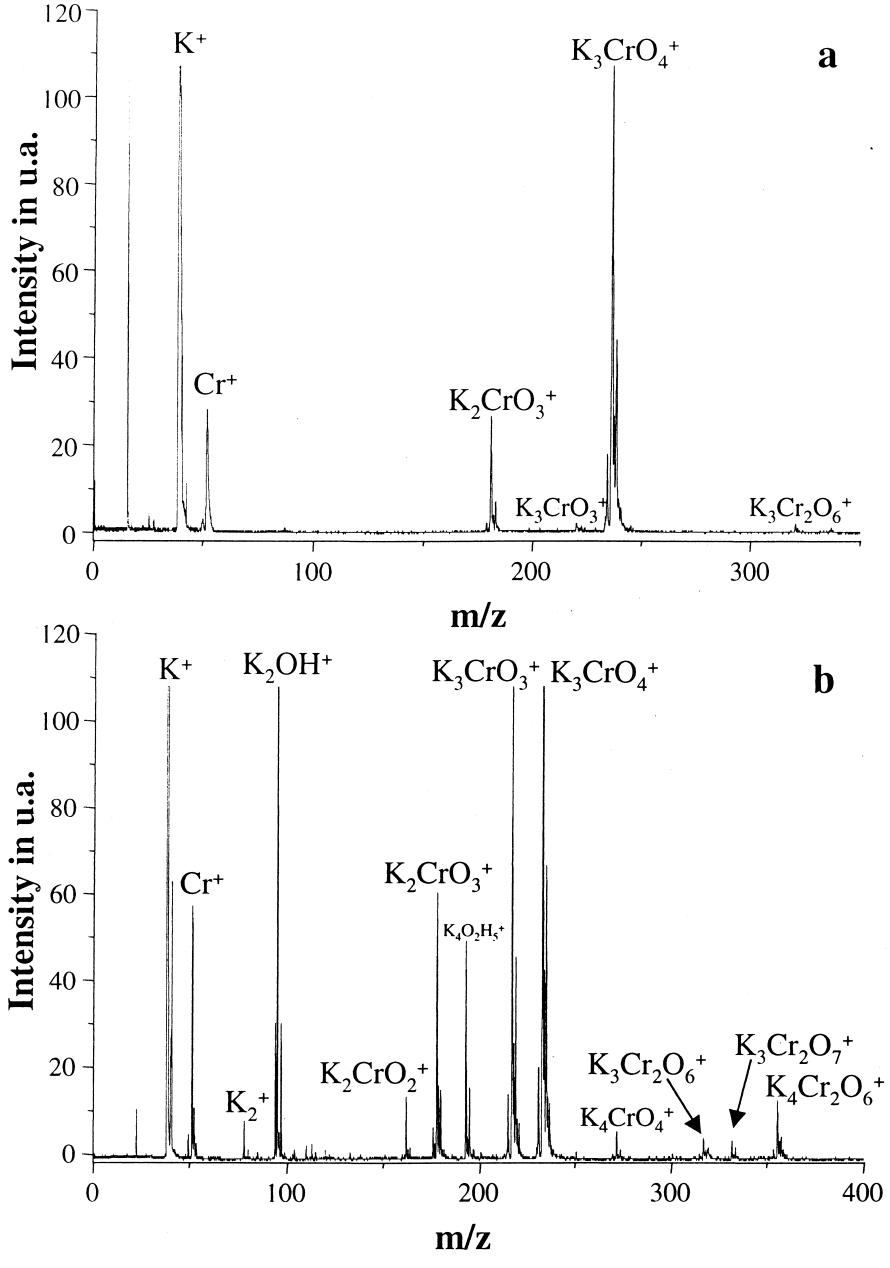

Fig. 7. Comparative TOF-LMMS study of (a) potassium bichromate and (b) chromate, at wavelength 357.9 nm.

wavelength. Experimentally, we observed a dramatic decrease of its absolute intensity when we compared the results obtained at 355 and 193 nm [Fig. 2(a) and 2(b)]. This behavior could not be satisfactorily accounted for by the increase of molecular fragmentation at 193 nm. As opposed to the first aggregation process, the second one is more adequate to account for the wavelength/behavior correlation. The accumu-

lation of counter evidence can be considered as sufficiently firm ground to allow for a rejection of the hypothesis of the first aggregation pathway.

3.2.3. Third hypothesis: aggregative process by successive adduction of neutral MO species to the CrO^+ ion:

$$CrO^+ \xrightarrow{MO} MCrO_2^+ \xrightarrow{MO} M_2CrO_3^+ \xrightarrow{MO} M_3CrO_4^+$$

In this process, the production of $M_3CrO_4^+$ ion stems probably from the adduction of successive neutral MO species to the precursor ion CrO^+ reaction (3). This hypothesis is supported by the systematic presence of $M_2CrO_3^+$ ions on the fingerprints of alkali chromate whatever the power density (Fig. 1). The poor abundance $MCrO_2^+$ ion was detected on the lithium and sodium chromate mass spectra at high power density [1].

Contrary to what observed in the process described by reaction (2), all ions included in this pathway are positive ions; consequently, their presence in the FTICR cell is not submitted to trapping potential restrictions.

Moreover, the significant decrease in $M_3CrO_4^+$ ion intensity when these compounds are successively studied at 355 and 193 nm [Figs. 2(a) and 2(b)] may be accounted for by this process. The dissociative energy of the LiO, NaO, KO, RbO, and CsO neutral species are, respectively, equal to 3.46 ± 0.17, 2.65 ± 0.17, 2.88 ± 0.22, 2.64 ± 0.87, and 3.07 ± 0.65 eV [21]. At 355 nm, the energy supplied by each photon is equal to 3.49 eV; it is 6.42 eV at 193 nm. The MO dissociation processes are also more active at 193 nm. This consideration can also give support to account for the very low absolute intensity of $M_3CrO_4^+$ ions at 355 nm under high power density conditions. The greater photon density, in the latter case, induced by a power density increase, favors the absorption of two photons required for the dissociation of most MO neutral molecules.

However, the dependency of behavior on wavelength may be also partially assigned to the stability of $M_3CrO_4^+$ ions when comparing results obtained first at 193 and 355 nm wavelengths, and second at high and low power density values. Thus, the cluster aggregation processes may be considered as a series of equilibria

$$CrO^+ \overset{MO}{\rightleftharpoons} MCrO_2^+ \overset{MO}{\rightleftharpoons} M_2CrO_3^+ \overset{MO}{\rightleftharpoons} M_3CrO_4^+ \quad (9)$$

where the ultimate step in FTICRMS experiments is the formation of the $M_3CrO_4^+$ ion.

At high power density or at more energetic wavelength (193 nm), the internal energy of $M_3CrO_4^+$ is important. This is why bounding breaks occur in the ionic structure and induce reverse processes, permitting the formation of more $MCrO_2^+$ and $M_2CrO_3^+$ ions (Figs. 1 and 4). Indeed, the detection of many $M_2CrO_3^+$ ions at 355 nm under high power density and the fact that the $Na_2CrO_3^+$ ion is the preponderant ion at 193 nm when studying sodium chromate for middle range values of the power density, seem to confirm the occurrence of reverse processes.

The identification of the $M_3CrO_4^+$ ion formation pathway allowed us to assess the importance of relative stability of ion clusters on the mass spectra obtained, in particular, when investigating the alkali chromate—alkali nitrate mixture. For that purpose, we investigated a complex mixture including, in particular, chromium and sodium species: technical grade magnesium chromate.

3.2.4. Study of the technical grade magnesium chromate—stability considerations

With a view to determining the pollutants and their relative importance, we investigated technical grade magnesium chromate by x-ray fluorescence and absorption atomic spectroscopy (Table 3). The results clearly indicate that this compound is very impure. Its mass spectrum is shown in Fig. 8(a); we compared it with that obtained with sodium chromate under the same experimental conditions [Fig. 8(b)].

The majority of cluster ions observed on the fingerprint of technical grade magnesium chromate are identical to those of sodium chromate and are made up of $Na_nCr_xO_y^+$ cluster ions. None of the cluster ions observed on the mass spectra of pure

Table 3
X-ray fluorescence and atomic absorption spectrometric analysis of technical-grade magnesium chromate

Species[a]	Na_2O	MgO	Al_2O_3	SiO_2	CaO	CrO_3	PbO
Relative abundance in percentage	15.4[b]	12.5[c]	0.90[c]	0.50[c]	9.00[c]	38.00[c]	3.9[c]

[a] Results are expressed in terms of an amount of oxide.
[b] AAS measurement.
[c] X-ray fluorescence results.

pentahydrate or anhydride magnesium chromate [Figs. 9(a) and 9(b), respectively] was detected. However, we did detect Na^+ (*m/z* 23), Al^+ (not shown), Ca^+ (*m/z* 40), Sr^+ (*m/z* 86, 87, and 88), and Pb^+ (*m/z* 206, 207, and 208) ions [Fig. 9(a)].

The fingerprint of this impure material surprisingly corresponds to that of pure chromate sodium, whereas sodium, magnesium, and calcium species are in similar proportions in technical grade magnesium chromate. The difference in Pauling electronegativity between first oxygen and sodium (2.51), and second between oxygen and magnesium (2.13), or oxygen and calcium (2.44) [1] did not account for the fact that no calcium–chromium–oxygen or magnesium–chromium–oxygen ions could be detected. To have a better understanding of this result, we may call for the concept of mixed cluster ion stability. It was shown previously that the cluster ions formed after alkali or alkaline earth chromate laser ablation are formed by ion/molecule reactions in the plume. The distribution of cluster ions may be correlated to some thermodynamic data: the affinity of oxygen counter ions and, above all, the thermodynamic stability of cluster ions. We demonstrated previously [1] that the FTICR mass spectrum is an indicator of the most stable ions. As a consequence, we will try to assess the difference in relative stability between oxygenated mixed cluster ions of alkali and alkaline earth chromium.

Kinne and co-workers [22,23] developed a simple model to evaluate the stability of oxygenated antimony and bismuth cluster ions. The special stability of some specific cluster ions may be accounted for by considerations of simple valence bond. The assignment of an oxidation number to all atoms present in the cluster ion structure allowed these authors to determine the most stable cluster ion: only such structures with a balanced number of free valence electrons (V_{el}) are stable. They distinguished two types of free valence electrons: the first ones are carried by the metal atoms and may be named metal free valence electron V_{el}(metal); the second ones by oxygen, they are oxygen free valence electron V_{el}(oxygen). When studying $M_mO_n^{q+}$ ions, if x is the oxidation number of metal M, the number of metal and oxygen free valence electrons are given, respectively, by

$$V_{el}(\text{metal}) = mx - q \quad (10)$$

$$V_{el}(\text{oxygen}) = 2n \quad (11)$$

The more stable ions have the same numbers of metal and oxygen free valence electron.

If we try to apply this model to the study of the mixed metal cluster ions obtained by laser ablation of alkali and alkaline earth chromate compounds, we might be able to predict their relative stability.

To conduct this study, we considered only the most intense ions observed on the fingerprints of alkali and alkaline earth—respectively, the $M_3CrO_4^+$ and the $M'_2CrO_4^+$ ionic structures [1]. The most common oxidation numbers for chromium are +III and +VI; the oxidation numbers for oxygen, alkali and alkaline earth compounds are respectively −II, +I, and +II. The results of calculation are summarized in the Table 4.

These results clearly show a greater stability of the $M_3CrO_4^+$ ion as compared to that of $M'_2CrO_4^+$. This explains why no alkaline earth chromium oxygenated

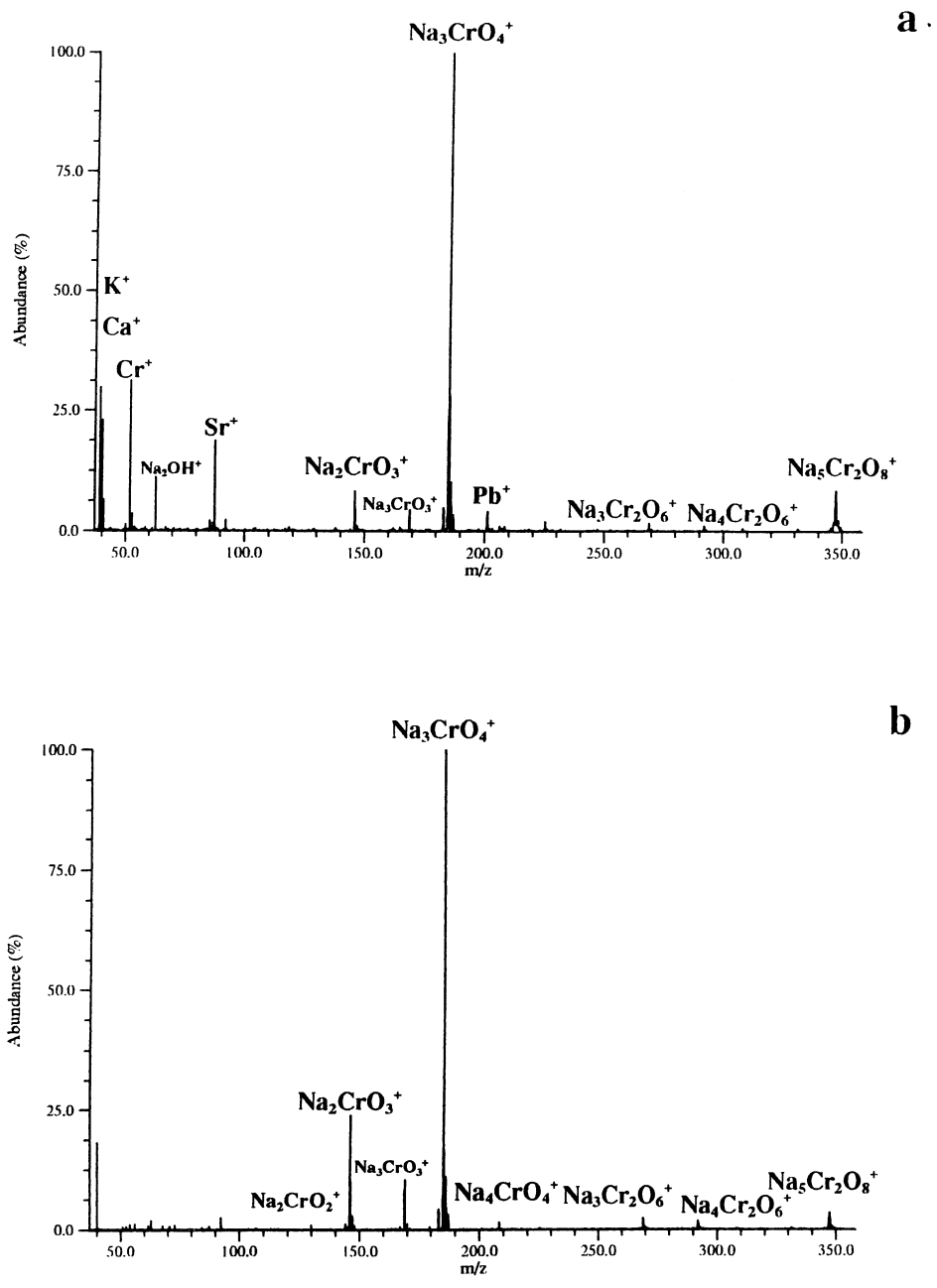

Fig. 8. Comparative FTICRMS study of (a) technical-grade magnesium chromate and (b) analytical grade sodium chromate at wavelength 355 nm.

ions was observed on the fingerprint of the technical grade magnesium chromate. Moreover, the oxidation number of chromium in these ionic structures seems to be six.

In general terms, the ion formation process occurring during the laser ablation of chromate compounds is strongly dependent on various parameters. The first one is the size of the counter ion which enhanced the

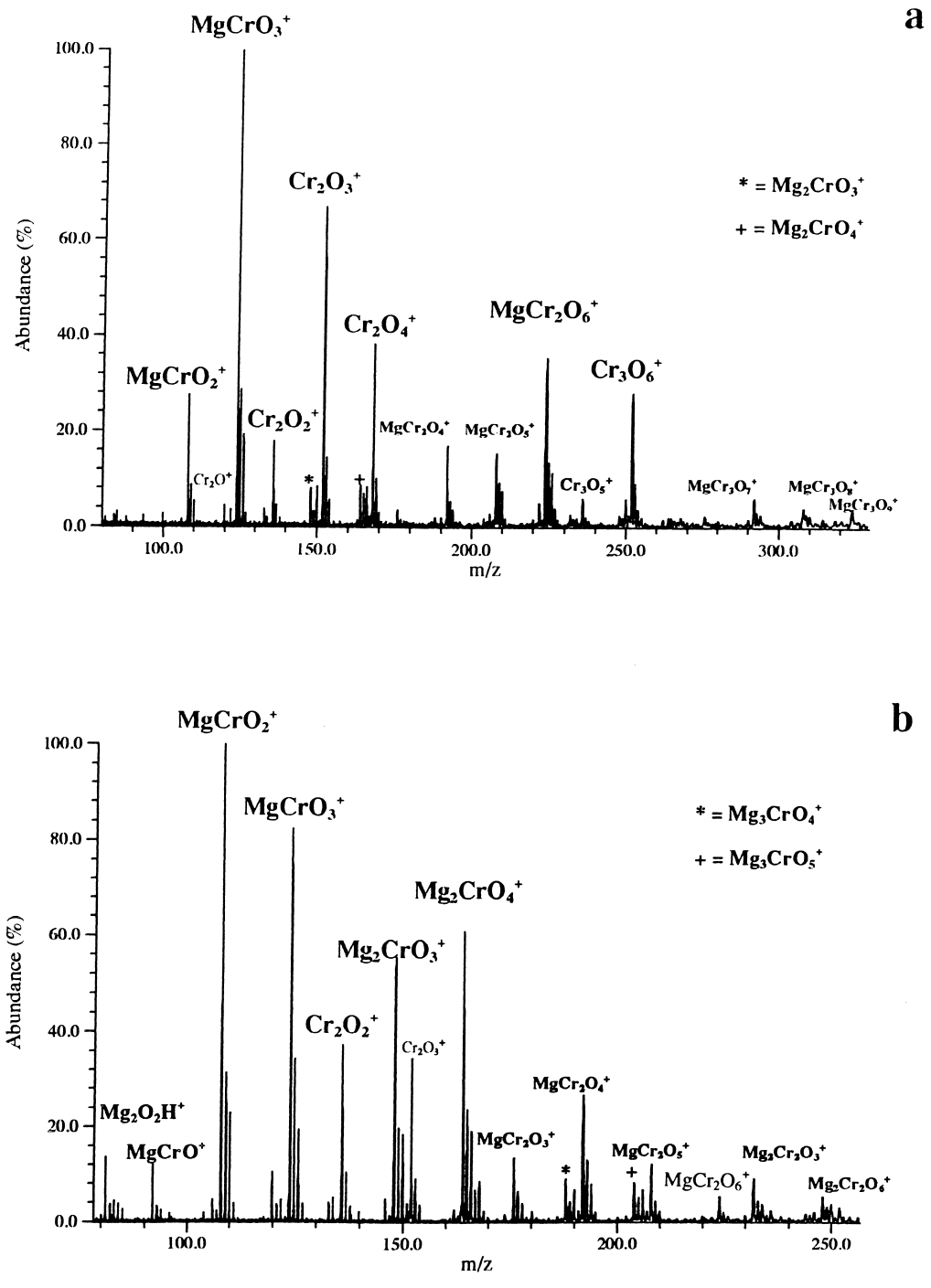

Fig. 9. Comparative FTICRMS fingerprints obtained for (a) pentahydrate and (b) anhydride magnesium chromate, at wavelength 355 nm.

Table 4
Number of free valence electrons (V_{el}) for oxygen and the metal atom (chromium and chromate counter ion) for the most intense ions observed when studying the alkali (M_2CrO_4) and alkaline earth ($M'CrO_4$) chromate compounds

	Alkali chromate		Alkaline earth chromate	
	$(MO)_3CrO^+$		$(M'O)_2CrO_2^+$	
Chromium valence	III	VI	III	VI
V_{el}(metal)	$3+3-1$	$6+3-1$	$3+2\times2-1$	$6+2\times2-1$
V_{el}(oxygen)	8	8	8	8
V_{el}(metal) − V_{el}(oxygen)	−3	0	−2	1

partition between stable and less stable ions [1]. The second one is the presence of other alkali or alkaline earth species, which may induce the appearance of other ion formation pathways and globally modify the fingerprint obtained.

Concerning the structure of $M_3CrO_4^+$ ions, the results obtained allow us to propose two 3-D structures.

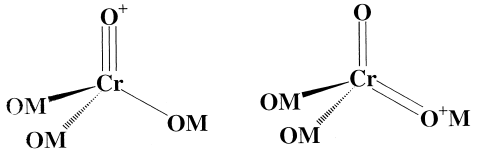

(12)

The fact that the oxidation number of chromium atom is six and $M_3CrO_4^+$ is formed by a stepwise adduction process suggests that the structure could be tetrahedral or pseudotetrahedral and looks like that of the chromate anion.

As opposed to oxides corresponding to simple binary systems, the chromate compounds have ternary systems. Laser ablation induces the formation of various neutral species which may be involved in ion/molecule reaction processes. Investigating this possibility will be done by a comparative study of hydrated and anhydride magnesium chromate compounds.

3.3. Influence of hydration on the fingerprint of magnesium chromate—understanding of the cluster ion formation in the study of alkaline earth chromate

3.3.1. FTICRMS study of hydrated and anhydride magnesium chromate

To undertake this part of the study, we selected two types of magnesium chromate compounds: yellow pentahydrate magnesium chromate and the ocher anhydride compound obtained by heating pentahydrate for 24 h at 200 °C. Unfortunately, the pentahydrate lost a part of lattice water in vacuum at a pressure of 10^{-6} Pa and turned orange. In fact, we did not investigate the original chromate but rather an intermediate hydrated compound whose degree of hydration is between that of anhydride and pentahydrate [Fig. 9(b)]. The number of water molecules in the crystalline lattice greatly influences the processes of ion cluster formation by a modification of the chromium/oxygen ratio.

The FTICR fingerprint of magnesium chromate is strongly dependent on the presence of water in the crystalline lattice [Figs. 9(a) and 9(b)]. The fingerprint of anhydride magnesium chromate described in detail in part I of the present work [1] is dramatically modified when the hydrated compound is investigated by FTICRMS. We could observe: (1) an increase of the pure chromium oxygenated cations paired in particular with the presence of additional ions $Cr_3O_5^+$ and $Cr_3O_6^+$ and an increase of $Cr_2O_x^+$ cluster ions ($x = 1$–4); (2) a reversing of the $MgCrO_2^+$–$MgCrO_3^+$ profile though the intensity of the former was higher than the latter, in the case of anhydride compound, the introduction of water into the crystalline lattice induced an increase of the intensity of $MgCrO_3^+$ cluster ions; (3) a decrease of the $MgCr_2O_4^+/MgCr_2O_6^+$ ratio when anhydride and hydrated chromate were successively investigated; (4) a modification of the distribution of the mixed cluster metal ions following the introduction of hydrated chromate, whereas these ions generally display an ionic structure with an equal number of magnesium and chromium atoms or an excess of magnesium atoms, the major part of the ions

observed when investigating hydrated chromate displayed an excess of chromium atoms, this can illustrated by the presence of $MgCr_3O_x^+$ ionic structures ($x = 7$–9) on the fingerprint of hydrated magnesium chromate.

In general terms, an increase of the oxygen/chromium ratio in the magnesium chromate compound studied induces an increase in the production of neutrals or ionic chromium species in the laser plume; this is related to a strengthening of their presence in the aggregation processes. Thus, cluster ions with a higher amount of chromium in their structure were observed on the fingerprint of the hydrated magnesium chromate compound.

3.3.2. Processes of ion formation in the study of alkaline earth chromate

As in the case of alkali chromate compounds, we may consider that the cluster ions are provided by sequential adduction of neutral molecules on precursor ions. As for alkaline earth chromate, the main two ion cluster series may be written by the formula $(MO)_nCrO^+$ and $(MO)_nCrO_2^+$, with $n = 1$–5 [1]. The cluster in each series are indeed separated by a mass equal to the MO weight. We may assume that the majority of cluster ions observed after laser irradiation of alkaline earth chromate compounds, by analogy with the behavior of alkali chromate, are formed by a stepwise adduction of MO neutral species on the two precursor species CrO^+ and CrO_2^+. The aggregation schemes are described by

$$CrO^+ \xrightarrow{MO} MCrO_2^+ \xrightarrow{MO} \ldots M_nCrO_{n+1}^+ \qquad (13)$$

$$CrO_2^+ \xrightarrow{MO} MCrO_3^+ \xrightarrow{MO} \ldots M_nCrO_{n+2}^+ \qquad (14)$$

In the case of the anhydride magnesium chromate compound, these aggregation pathways are well adhered to, whereas some changes appear when studying the pentahydrate compound. In the latter case, the ions described in the expressions (13) and (14) are less numerous. The number of MO neutral adducts on the CrO^+ and CrO_2^+ is lower. At the same time, the number and relative intensity of cluster ions with more than one chromium atom in their structure increases dramatically [Fig. 9(a) and 9(b)]. These results suggest that we have competitive processes: an adduct of either an alkaline earth or of a chromated neutral species onto the precursor ions. The introduction of water molecules into the crystalline lattice of the magnesium chromate compounds induces an increase in the number of neutral chromium species in the gaseous cloud above the analyte after laser irradiation of the compound. An accurate study of the fingerprint of magnesium chromate reveals that two kinds of neutral chromium species may be involved in the aggregation process: CrO_2 and CrO_3 molecules.

In general terms, for a given precursor ion $M_nCr_xO_y^+$, three aggregation processes may be assumed, involving an adduct of MO, CrO_2, or CrO_3 neutral species

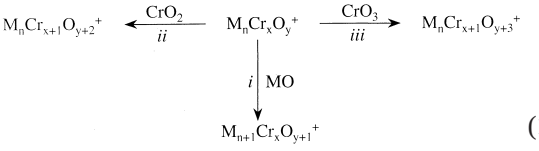

(15)

The result of the aggregation process is governed by (1) the relative ratio of alkaline earth neutrals to chromated ones in the gaseous cloud above the surface of the analyte after laser ablation: and (2) the relative affinity of the various neutrals (MO, CrO_2, and CrO_3) with the precursor ion. It appeared clearly that an increase of oxygen atoms in the compound studied is favorable to the *ii* and *iii* processes described on diagram (15). In the same way, an increase of MO units in the precursor $M_nCr_xO_y^+$ ion induces a greater yield of ions, along the same lines.

As opposed to this, the comparative study of all alkaline earth chromate shows that an increase of the radius of the counter ions restrains the production of cluster ions by the processes *ii* and *iii* at low values of *n*. The $MgCrO_4$ compound yields indeed [1] $MgCr_2O_4^+$, $MgCr_2O_5^+$, and $MgCr_2O_6^+$ cluster ions, whereas the first ions with at least two chromium

atoms, as detected on the fingerprint of barium chromate, are $Ba_2Cr_2O_5^+$; $Ba_2Cr_2O_6^+$; and $Ba_2Cr_2O_7^+$. The production of $BaCr_2O_x^+$ with $x = 4–6$, after laser irradiation of the barium chromate compound, was never observed

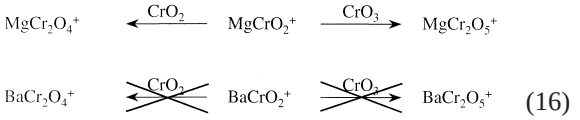

(16)

In general terms, the ions present on the fingerprints of alkaline earth chromate result from aggregative processes on precursor ions. The relative yield of cluster ions according to the three different aggregation reactions *i*, *ii*, and *iii* in diagram (15) are governed by (1) the ratio of chromated and alkaline earth neutral species; and (2) the relative affinity of the precursor ion to MO, CrO_2, and CrO_3 species. We may generalize this concept of competitive aggregative processes for a better understanding of all the clusters formed by laser ablation ionization of alkali earth chromate (Fig. 10).

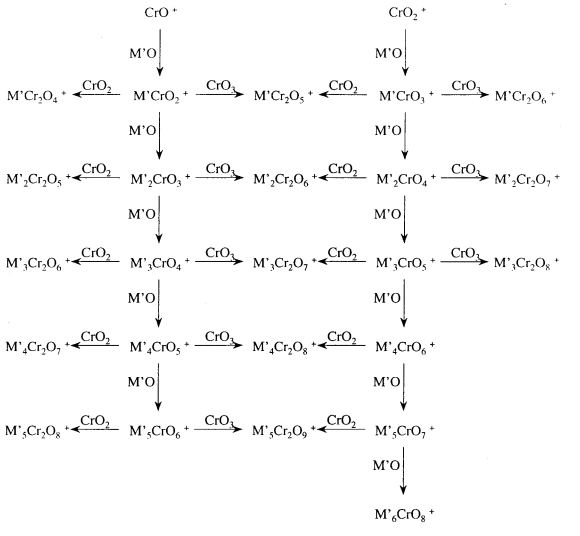

Fig. 10. Growing paths of alkaline earth–chromium–oxygen cluster ions after laser ablation.

4. Conclusion

The systematic study of alkali and alkaline earth chromate by two LMMS techniques (TOF-LMMS and LA-FTICRMS) offered an improved understanding of processes of ion formation.

When investigating these compounds, we provide evidence of the fact that the cluster ions formed by laser ablation/ionization are not the result of a combination between a neutral molecule of desorbed analyte and a charged species—in particular the counter ion of the chromate compound—but rather the result of a stepwise process. It was shown that, most probably, the cluster ions observed on the fingerprint of these two ranges of compounds (alkali and alkaline earth chromate) is formed by growing on the basis of smaller entities, in particular by a sequential addition of MO neutral molecules (where M is a alkali or an alkaline earth atom) on the Cr^+, CrO^+, and CrO_2^+ precursor ions.

The presence of various neutral species in the gaseous cloud, respectively, CrO_2, CrO_3, and MO makes the processes of ion formation more complex by involving competitive reaction pathways. As a consequence, the yield of a given ion is governed by the affinity of its precursor ion with the three kinds of neutral species. This affinity clearly depends, first on the radius of the counter ion (the greater it is, the higher the probability of having an MO adduct rather than a CrO_2 or a CrO_3 one), and second on the precursor ion $M_nCr_xO_y^+$ (a low *n* value is more conducive to an MO adduct).

Moreover, the high stability of the $M_3CrO_4^+$ species allowed us to propose two structures of the $M_3CrO_4^+$ ion, after considering a simple model based on the minimization of unpaired electrons; the latter phenomenon is favorable to a greater stability of the ion. Theoretical calculation is currently being done, first to check on their structure and find the most stable ionic structure, and second to confirm the stepwise growth of the cluster ions detected on the fingerprints of alkali chromate. However, the first results made it possible to highlight an increase in the dipole moment of the structures MO when the size of the alkaline atom increases. This led to an increase in

the ionicity of the connection and to repliment of the structure of the ion $M_3CrO_4^+$ when the $Li_3CrO_4^+$ and the $Na_3CrO_4^+$ ions are successively studied with in this last case obviousness of ONaO bridge.

These concepts are of prime importance for the speciation problem, considering that laser microprobe mass spectra does not allow for direct speciation diagnostics. The mass spectra obtained after laser irradiation of a complex analyte is not the superposition of the fingerprints of various mixed components, but rather the representation of the cluster ions formed by ion/molecule reactions between all the ionic and neutral species induced by laser ablation/ionization of these mixed components.

In conclusion, the simple comparison with the mass spectra in a database is not sufficient to indicate the presence of a given compound. The analysis of the results supplied by mass spectra is indeed much more laborious.

Acknowledgement

The authors gratefully acknowledge financial support from Ugine Savoie, and Gabriel Krier and Lionel Vernex-Losel for their technical support.

References

[1] Part I.
[2] F.P. Novak, K. Balasanmugan, K. Viswanadham, C.D. Parker, Z.A. Wilk, D. Mattern, D.M. Hercules, Int. J. Mass Spectrom. Ions Phys. 53 (1983) 135.
[3] B. Schueler, P.K.D. Feigl, F.R. Krueger, Z. Naturforsch. 37a (1983) 1078.
[4] F.R. Krueger, Z. Naturforsch. 38a (1983) 385.
[5] B. Jöst, B. Schueler, F.R. Krueger, Z. Naturforsch. 37a (1982) 18.
[6] J. Dennemont, J.C. Landry, Microbeam Analysis—1985, J.T. Armstrong, (Ed.), San Francisco Press Inc., San Francisco, 1985, p. 305.
[7] P.E. Lafargue, J.J. Gaumet, J.F. Muller, A. Labrosse, J. Mass Spectrom. 31 (1996) 623.
[8] J.K. Gibson, J. Appl. Phys. 78 (1995) 1274.
[9] A. Hachimi, E. Poitevin, G. Krier, J.F. Muller, M.F. Ruiz-Lopez, Int. J. Mass Spectrom. Ion Processes 144 (1995) 23.
[10] A. Hachimi, E. Million, E. Poitevin, J.F. Muller, Analusis 21 (1993) 11.
[11] X.H. Liu, X.G. Zhang, Y. Li, X.Y. Wang, N.Q. Lou, Int. J. Mass Spectrom. 177 (1998) L1.
[12] N. Chaoui, E. Million, J.F. Muller, Chem. Mater. 10 (1998) 3888.
[13] A. Mele, D. Consalvo, D. Stranges, A. Giardini-Guidoni, R. Teghil, Int. J. Mass Spectrom. Ion Processes 95 (1990) 359.
[14] I.H. Musselman, R. Linton, D.S. Simons, Anal. Chem. 60 (1988) 110.
[15] X.H. Liu, X.G. Zhang, Y. Li, X.Y. Wang, N.Q. Lou, Chem. Phys. Lett. 288 (1998) 804.
[16] X.H. Liu, X.G. Zhang, X.Y. Wang, N.Q. Lou, Int. J. Mass Spectrom. Ion Processes 171 (1997) L7.
[17] M. Pelletier, G. Krier, J.F. Muller, D. Weil, M. Johnston, Rapid Commun. Mass Spectrom. 2 (1988) 146.
[18] J.F. Muller, M. Pelletier, G. Krier, D. Weil, J. Campana, Microbeam Analysis—1989, P.E. Russell (Ed.), San Francisco Press Inc., San Francisco, 1989, p. 311.
[19] F. Aubriet, B. Maunit, B. Courier, J.F. Muller, Rapid Commun. Mass Spectrom. 11 (1997) 1596.
[20] E.B. Rudny, L.N. Sidorov, L.A. Kuligina, G.A. Semenov, Int. J. Mass Spectrom. Ion Processes 35 (1985) 95.
[21] J.R. Kerr, Chemical Rubber Compagny Handbook of Chemistry and Physics, 77th ed. D.R. Lide (Ed.), CRC Press, Boca Raton, FL, 1996.
[22] M. Kinne, T.M. Bernhardt, B. Kaiser, K. Rademann, Int. J. Mass Spectrom. Ion Processes 167/168 (1997) 161.
[23] B. Kaiser, M. Bernhardt, M. Kinne, T.K. Rademann, Int. J. Mass Spectrom. 177 (1998) L5.